

Journal Name

ARTICLE TYPE

Cite this: DOI: 00.0000/xxxxxxxxxx

Enhanced quantum properties of shallow diamond atomic defects through nitrogen surface termination - supporting information

Rotem Malkinson,^a Mohan Kumar Kuntumalla,^b Arsène Chemin,^c Tristan Petit,^c Alon Hoffman,^b and Nir Bar-Gill^{*a,d,e}

Received Date
Accepted Date

DOI: 00.0000/xxxxxxxxxx

Nitrogen vacancy (NV) centers in diamond have emerged in recent years as leading quantum sensors in various modalities. Most applications benefit from shallow NVs, enabling higher sensitivity and resolution. However, near-surface NVs (< 20 nm depth) suffer from reduced stability and coherence properties due to additional noise. We demonstrate a novel surface termination technique based on nitrogen plasma under non-damaging conditions, achieving significant improvement in NV optical stability and quantum coherence. X-ray characterization of the nitrogen-terminated diamond surface suggests limited charge transfer between the NV centers and surface electronic states compared to oxygen-terminated diamond

S1 Methods

For XPS and HREELS surface analyses, single crystal (100)-oriented diamonds (8 mm × 8 mm × 0.5 mm, ICDAT Ltd.) were used (these diamonds were not used for optical characterizations). The samples were cleaned in an ultrasonic bath for 10 minutes using acetone and ethanol followed by 4 μm thick homoepitaxial buffer layer growth in microwave chemical vapor deposition (MWCVD) (SEKI, 2.45 GHz, power 6000 W) system using hydrogen (H₂) and methane (CH₄) as precursor gases with a flow rate and gas pressure of 250:10 standard cubic centimeters per minute (sccm) (H₂:CH₄) and 150 Torr, respectively. The substrate temperature during growth was 900 °C. The buffer layer deposition was carried out at the Israeli Center of Advanced Diamond Technologies (ICDAT Ltd.).

The surface RF(N₂) plasma treatment and analysis were carried out in two UHV systems maintained at a base pressure of 5 × 10⁻¹⁰ Torr, as previously described. The UHV system-1 is

equipped with RF(N₂) plasma processing facility and the UHV system-2 is equipped with XPS and HREELS facilities.

Following the buffer layer deposition, the H-diamond (100) sample was transferred ex situ (exposed to ambient conditions) into UHV system-1. The diamond sample was mounted onto a custom-designed 2-in-1 sample holder and heater (Boralectric resistive heater) that facilitates in situ annealing. Next, the sample was vacuum annealed to 600 °C for 5 min, in order to induce desorption of adventitious ambient contaminants prior to the plasma exposure. Next, the diamond surfaces were examined by low energy electron diffraction (LEED), which render a (1x1) pattern for an incident electron beam energy as low as ~100 eV and a characteristic C(1s) XP line shape and related plasmon of diamond carbon were measured showing that the homoepitaxial layer is highly ordered and free of impurities within the sensitivity of our measurements. Subsequently, the as-conditioned surfaces were exposed to RF(N₂) plasma for 30 min at two different N₂ gas pressures: 3 × 10⁻² (damaging condition) and 7 × 10⁻² Torr (non-damaging condition), and at plasma power of 36 W. The RF processing setup consists of a non-line-of-sight plasma source described in detail previously^{S1}. After plasma exposure, the RF nitrated diamond (100) samples were transferred ex situ into UHV system-2 to carry out XPS and HREELS measurements to evaluate their surface chemical and structural properties.

The XPS measurements were performed using a non-monochromatic Mg Kα anode X-ray source (XR50, SPECS) at an incident angle of 55° from the surface normal and a hemispherical analyzer (PHOIBOS 100, SPECS). The incident X-ray photons energy line width was 0.68 eV, as per the source specifications provided by the manufacturer (SPECS, Germany). The XP spec-

^a Institute of Applied Physics, The Hebrew University of Jerusalem, Jerusalem 91904, Israel

^b Schulich Faculty of Chemistry, Technion – Israel Institute of Technology, Haifa 32000, Israel

^c Young Investigator Group Nanoscale Solid-Liquid Interfaces, Helmholtz Zentrum Berlin für Materialien und Energie GmbH, Berlin 12489, Germany

^d The Racah Institute of Physics, The Hebrew University of Jerusalem, Jerusalem 91904, Israel

^e The Center for Nanoscience and Nanotechnology, The Hebrew University of Jerusalem, Jerusalem 91904, Israel

* Corresponding author, E-mail: nir.bar-gill@mail.huji.ac.il

† Electronic Supplementary Information (ESI) available: [Additional experimental details including methods, optical setup, sample preparation and further data of optical FL scans and ODMR measurements]. See DOI: 00.0000/00000000.

tra were measured at room temperature (RT) in the 200-600 eV binding energy range to determine the chemical state of the nitride surfaces. In addition, high-resolution measurements were carried out in the N(1s) and C(1s) narrow spectral ranges. The pass energy and scan step used in the XPS measurements were 15 eV and 0.1 eV, respectively. To minimize the surface charging effects, a thin (100 μm) Molybdenum plate mask with a circular opening (diameter = 8 mm) was placed in contact with the sample surface and firmly connected to the sample holder's electrical ground. Curve-fitting of XPS peaks was performed after background subtraction as described by Shirley^{S2} and using a mixed Gaussian (Y%)-Lorentzian(X%) peak shape, defined in CasaXPS software (version 2.3.15) as GL(X%). The C(1s) and N(1s) peaks are suited to the default GL(30) peak shape^{S3,S4}. From these measurements, it was determined that no impurities were present on the H-diamond surface within the sensitivity of the XPS (~ 0.5 at.%). HREELS measurements were carried out using primary electron energy of 8.4 eV. The FWHM of the elastically scattered electron peak was 16 meV. The spectra were recorded up to loss energies of 500 meV in the specular geometry at an incident angle of 55° from the surface normal. All spectra were recorded in situ at RT under UHV conditions after annealing to 300 $^\circ\text{C}$. The curve-fitting of the HREEL spectra was performed by means of XPSPEAK (version 4.1) software.

S2 Diamond Preparation for Optical Studies

For optical studies, electronic grade single crystal diamond (100) (1.6 mm \times 1.6 mm \times 0.1 mm, Element Six, UK) was implanted (Innovion) with ^{15}N ions at an energy of 2 keV and a dose of 5×10^{10} [$\frac{\text{ions}}{\text{cm}^2}$]. The diamond was then boiled in tri-acid ($\text{HNO}_3:\text{H}_2\text{SO}_4:\text{HClO}_4$ - 1:1:1) mixture for 1 hour at 180 $^\circ\text{C}$ and then annealed to 1200 $^\circ\text{C}$ following the steps in ref.^{S5}. The diamond was subsequently boiled in tri-acid again.

For oxygen termination, the diamond was then treated with piranha solution ($\text{H}_2\text{SO}_4:\text{H}_2\text{O}_2$ - 3:1) for 10 min.

Preparing the diamond for the nitrogen RF plasma, the diamond was boiled in a tri-acid ($\text{HNO}_3+\text{H}_2\text{SO}_4+\text{HClO}_4$) mixture for 30 min at 140 $^\circ\text{C}$, followed by boiling in water for 30 min to remove non-diamond species from the diamond surface if any. Next, the diamond sample was placed onto a custom-designed 2-in-1 sample holder and heater with a molybdenum mask having a circular opening (diameter = 1.5 mm) and transferred into UHV system-1 to carry out RF(N_2) plasma treatment. Prior to plasma nitridation, the sample was vacuum annealed to 800 $^\circ\text{C}$ for 5 min to remove oxygen impurities. Then, the sample was exposed to non-damaging RF(N_2) plasma for 30 min as described above and the sample was taken out without any further processing to perform optical measurements.

After these measurements, the same sample was boiled in tri-acid as described above, followed by vacuum annealing to 800 $^\circ\text{C}$ for 5 min and exposed to damaging RF(N_2) plasma for 30 min as described above.

S3 Optical Setup

Optical fluorescence and quantum spin properties were measured using a home-built confocal microscope. A 532 nm pulsed laser

(KATANA-05, 50 ps pulse) is used for NV excitation and pumping through a Nikon oil objective (Plan Apo λD 60x/1.4), the spot size is diffraction limited at ~ 200 nm. Readout FL is collected using an Excelitas single photon counter module (SPCM, SPCM-780-13-FC). The laser was operated at 1.9 mW (average intensity power), the diamond was placed on a cover slip on top of the objective. Oil (Nikon immersion oil type A, refractive index $n = 1.515$) was used only between the cover slip and the objective. Schematics of the setup are shown in Figure S1.

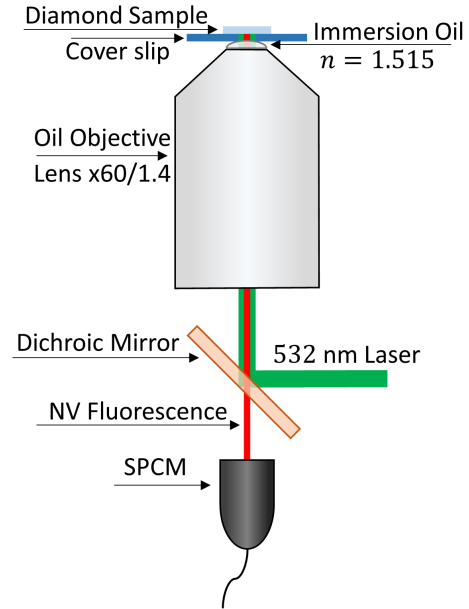


Fig. S1 Optical setup schematics. A 532 nm laser is used to excite NVs through an oil objective. Immersion oil (refractive index $n = 1.515$) is used between the objective and the glass coverslip for index matching. NV fluorescence is subsequently collected using a SPCM. The green laser and red emission are split using a dichroic mirror.

S4 ODMR effects and fluorescence dynamics

During the fluorescence measurement of the non-damaging termination, we noticed unexpectedly high NV concentrations. The implantation parameters were chosen so as to create single NVs. However, the electron spin resonance (ESR) measurements revealed multiple resonant frequencies (Figure S2(a)). Given that each pair of resonance frequencies is attributed to a different NV orientation, we expect four possible pairs for a single crystal diamond sample according to the four possible orientations of NVs (Figure S2(b)). However, certain spots result in ESR scans that fit to 6 different orientations (Figure S2(a)). In such rare occasions, ESR measurements show the resonance of all the dips are magnetic dependent and the spectral separation between the dips is in the order of MHz (approx. 15 MHz in the measurement shown in Figure S2(a)). We therefore attribute this phenomenon to local stress induced on the NV ensemble due to close proximity to the diamond surface, or to stronger coupling to local nuclear spins (with some dependence on the angle of coupling vs. the external field).

In addition, Figure S3 depicts a change in NV fluorescence

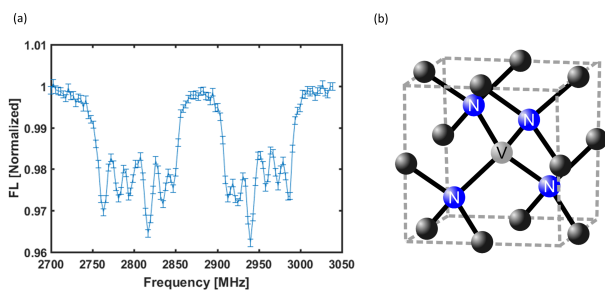


Fig. S2 (a) ESR spectra taken from a fluorescent spot in a non-zero external magnetic field. (b) The possible orientations for an NV in a diamond. Each orientation contributes two resonant frequencies, associated with the ± 1 spin states. As seen from (b) we expect to see up to 4 orientations (8 dips), but we see in (a) 12 dips.

observed due to repeated scans. We noticed variations in fluorescence intensity of NVs following different measurement sequences. Usually, the NV emitted count rate would increase after running ESR and Rabi on the FL spot, while the FL in the surrounding area decreased. On fewer occasions, we noticed the opposite phenomena – the central FL spot dimmed, while the FL of the surrounding area increased.

This phenomenon of intensity change in a FL spot persisted after annealing the diamond for 30 minutes at both 300 °C and 400 °C. Furthermore, the change in fluorescence intensity reaches a permanent steady state in which the count rate remains constant with any subsequent measurement sequence.

All measurements were taken after reaching the new steady state.

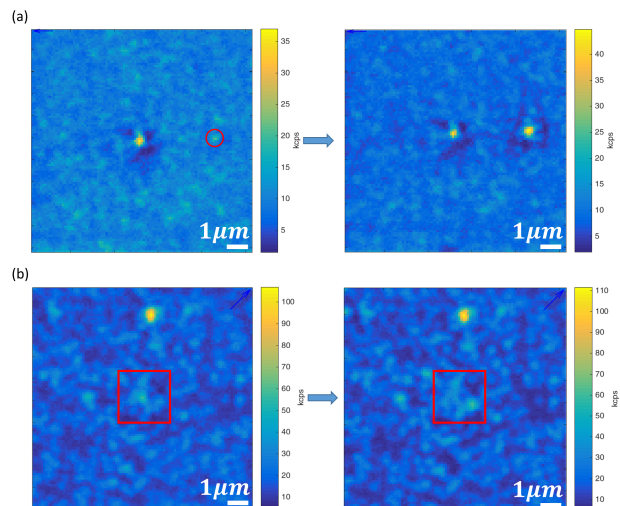


Fig. S3 (a) FL spot fluorescence increases after running measurements on it. The red circle in the left scan depicts the FL spot which is going to be measured. The right scan shows how the fluorescence intensity changes at the FL spot and its surrounding area. (b) The left scan was taken before starting to measure the FL spot in the center of the square. The right scan shows how the fluorescence map changed after measurements. It can be seen that the center FL spot disappeared, while the surrounding area's fluorescence intensity increased.

Notes and references

- 1 M. Attrash, M. K. Kuntumalla and A. Hoffman, *Surface Science*, 2019, **681**, 95–103.
- 2 D. A. Shirley, *Physical Review B*, 1972, **5**, 4709–4714.
- 3 M. C. Biesinger, B. P. Payne, A. P. Grosvenor, L. W. M. Lau, A. R. Gerson and R. S. C. Smart, *Applied Surface Science*, 2011, **257**, 2717–2730.
- 4 M. C. Biesinger, L. W. M. Lau, A. R. Gerson and R. S. C. Smart, *Applied Surface Science*, 2010, **257**, 887–898.
- 5 S. Sangtawesin, B. L. Dwyer, S. Srinivasan, J. J. Allred, L. V. H. Rodgers, K. De Greve, A. Stacey, N. Dontschuk, K. M. O'Donnell, D. Hu, D. A. Evans, C. Jaye, D. A. Fischer, M. L. Markham, D. J. Twitchen, H. Park, M. D. Lukin and N. P. de Leon, *Physical Review X*, 2019, **9**, 031052.